



European Space Research
and Technology Centre
Keplerlaan 1
2201 AZ Noordwijk
The Netherlands
Tel. (31) 71 5656565
Fax (31) 71 5656040
www.esa.int

DOCUMENT

EChO wavelength coverage & spectral resolving power

Document leads: G. Tinetti, P. Drossart, P. Hartogh
with input from T. Encrenaz & M. Tessenyi

Prepared by: Giovanna Tinetti, Pierre Drossart, Paul Hartogh, with inputs from T. Encrenaz and M. Tessenyi

Reference

Issue 1

Revision 0

Date of Issue 16th December, 2013

Status

Document Type

Distribution

European Space Agency
Agence spatiale européenne



APPROVAL

Title EChO wavelength coverage and spectral resolving power	
Issue 1	Revision 0
Author Giovanna Tinetti, Pierre Drossart, Paul Hartogh with inputs from T. Encrenaz and M. Tessenyi, and the EChO SST	Date
Approved by	Date

CHANGE LOG

Reason for change	Issue	Revision	Date

CHANGE RECORD

Issue	Revision		
Reason for change	Date	Pages	Paragraph(s)



Table of contents:

1 Introduction 4

2 The 1 – 16 μm range 6

 2.1 The 2 – 16 μm range6

 2.2 The 1 – 2 μm range.....8

 2.3 The 1 – 16 μm range8

3 Wavelengths less than 1 μm 9

4 Conclusions.....10

5 References.....11

6 Appendix.....13

1 INTRODUCTION

EChO will observe between 150 and 300 planets, including objects with sizes ranging from the super-Earth to the Jupiter-size, and temperatures between temperate ($\sim 300\text{K}$) and very hot (e.g. reaching temperatures close to 3000K , such as KOI-13b, HAT-P-7b, WASP-12b, WASP-18b etc.). To maximise the scientific impact of the mission, we need to ensure that all the key spectral features characterising the physical and chemical conditions of planetary atmospheres can be accessed. It is also critical that we can observe planets at different temperatures (nominally from 300 K to 3000 K , see Fig. 1-1), to probe the differences in the chemistry, potentially linked to different formation and evolution scenarios. Additionally, the visible part of the spectrum will be used to measure the planetary albedo, detect Rayleigh scattering/cloud contributions and also monitor simultaneously the stellar activity to remove/mitigate its impact on the observations (see Ribas, Micela, Tinetti, TN). This means covering the largest wavelength range feasible from the visible to the Mid-IR, i.e. ~ 0.55 to $11\text{ }\mu\text{m}$ (possibly $0.4\text{--}16\text{ }\mu\text{m}$).

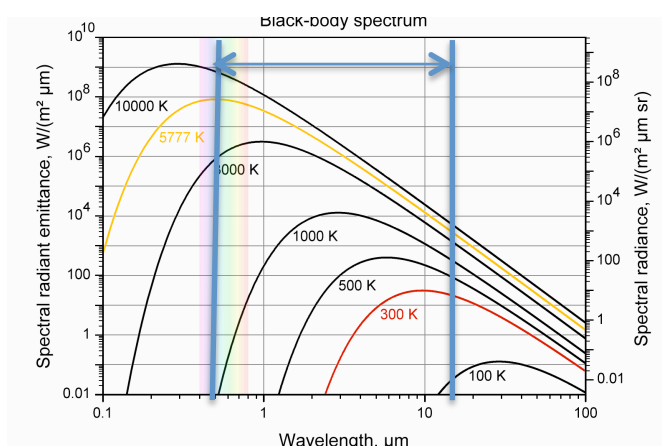


Fig. 1-1: Blackbody curves corresponding to different temperatures: the colder the temperature, the longer the wavelengths were the Planckian curves peak. The two blue lines show optimal wavelength range to characterise planets from 300 K to 3000 K .

In Table 1 we list the key atomic and molecular species expected in exoplanetary atmospheres. Molecular species such as H_2O , CH_4 , CO_2 , CO , NH_3 are essential to understand the chemistry of those planets (Moses et al., 2011; Venot et al, 2012, 2013), but also more exotic species present in Brown Dwarf atmospheres should be sought for (e.g. metal oxides and hydrides, TiO , VO , TiH , FeH etc., see Allard, TN). The broad wavelength coverage guarantees that all the aforementioned species and many others can be detected in multiple spectral bands (see Tennyson & Yurchenko, TN), even at low SNR, optimising their detectability in atmospheres at different temperatures.

Redundancy (i.e. molecules detected in multiple bands of the spectrum) significantly improves the reliability of the detection, especially when multiple chemical species overlap in a particular spectral range. Bands of different intensities also probe different atmospheric levels, giving insight into the vertical distribution of the observed species. Thus, said redundancy in molecular detection is also necessary to allow the retrieval of the vertical thermal structure and molecular abundances (e.g. Goody & Yung, 1989). Redundancy can be guaranteed only through a broad spectral coverage and appropriate SNR.

In the following sections, we review the importance of different spectral regions in the goal $0.4\text{--}16\text{ }\mu\text{m}$ wavelength range.

	0.4-1 μm	1-5 μm	5-11 μm	11-16 μm
<i>R, baseline</i>	300	300	≥ 30	30
<i>R, desired</i>	300	300	300	300
<i>Species</i>				
*H ₂ O	0.51, 0.57, 0.65, 0.72, 0.82, 0.94	1.13, 1.38, 1.9, 2.69	6.2	continuum
*CO ₂	-	1.21, 1.57, 1.6, 2.03, 4.25	-	15.0
C ₂ H ₂	-	1.52, 3.0	7.53	13.7
HCN	-	3.0	-	14.0
C ₂ H ₆	-	3.4	-	12.1
O ₃	0.45-0.75 (the Chappuis band)	4.7	9.1, 9.6	14.3
HDO	-	2.7, 3.67	7.13	-
*CO	-	1.57, 2.35, 4.7	-	-
O ₂	0.58, 0.69, 0.76, 1.27	-	-	-
NH ₃	0.55, 0.65, 0.93	1.5, 2, 2.25, 2.9, 3.0	6.1, 10.5	-
PH ₃	-	4.3	8.9, 10.1	-
*CH ₄	0.48, 0.57, 0.6, 0.7, 0.79, 0.86,	1.65, 2.2, 2.31, 2.37, 3.3	6.5, 7.7	-
CH ₃ D	?	3.34, 4.5	6.8, 7.7, 8.6	-
C ₂ H ₄	-	3.22 , 3.34	6.9, 10.5	-
H ₂ S	-	2.5, 3.8 ...	7	-
SO ₂	-	4	7.3 , 8.8	-
N ₂ O	-	2.8, 3.9, 4.5	7.7, 8.5	-
NO ₂	-	3.4	6.2 , 7.7	13.5
H ₂	-	2.12	-	-
H ₃ ⁺	-	2.0, 3-4.5	-	-
He	-	1.083	-	-
*Na	0.589	1.2	-	-
*K	0.76	-	-	-
TiO	0.4-1	1-3.5	-	-
VO	0.4-1	1-2.5	-	-
FeH	0.6-1	1-2	-	-
TiH	0.4-1	1-1.6	-	-
Rayleigh	0.4-1	-	-	-
Cloud/haze	yes	possible	silicates, etc.	-
H H α	0.66			
H H β	0.486			
Ca	0.8498, 0.8542, 0.8662		-	-

Table 1: Main spectral features between 0.4 and 16 μm , the goal wavelength coverage considered for EChO. The asterisk indicates the molecular/atomic species already detected in the atmospheres of exoplanets. At wavelengths shorter than 2 μm spectroscopic data are often not complete, so that the use of this region is much more difficult for band identification and analysis. The main bands are illustrated in bold.

2 THE 1 – 16 μM RANGE

2.1 The 2 – 16 μm range

From a molecular perspective, with some exceptions, wavelengths longer than 2 μm are the best suited for detection because:

- (1) spectral signatures are stronger, as all molecules have their fundamental vibration-rotation bands in this range;
- (2) in eclipse observations the planet to star flux ratio increases at longer wavelengths;
- (3) at wavelengths shorter than 2 μm , spectroscopic data for molecules –overtone and combination bands– are usually much less well known, especially at high temperature.

Most molecules in Table 1 exhibit two or more strong molecular bands in the 2 -16 μm range, so both redundancy and the ability to retrieve a vertical structure are guaranteed. The exceptions are represented by molecules with strong electronic transition rather than rotation and vibration modes, i.e. metal hydrides and oxides (see Fig. 2-3), molecular oxygen etc.

For an unambiguous identification of a given molecule, the spectral resolving power should, ideally, be sufficient to separate two adjacent J-components of this molecule (Fig. 2-1). This interval is equal to $2 B_0$, where B_0 is the rotational constant of the molecule. Table 2 lists this interval $\Delta\nu$ for the main bands of our list of candidate species, and the resolving power required to resolve this interval. Two spectral domains are considered, the 2 – 5 μm and the 5 – 16 μm range. The molecular features, in fact, become stronger and less packed at wavelengths longer than 5 μm . The spectral separation of molecular bands longward 5 μm is easier than at shorter wavelengths, because the overlap is less severe. We can see that for H_2O , CH_4 and their isotopes, as well as for NH_3 and PH_3 , a resolving power of 300 (shortward 5 μm) and ~150 (longward 5 μm) is sufficient for identifying the bands unambiguously at any temperature.

Molecule	$\Delta\nu=2B_0$ cm^{-1}	ν (S max) 2–5 μm	S max $\text{cm}^{-2} \text{am}^{-1}$	R 2–5 μm	ν (S max) 5–16 μm	S max $\text{cm}^{-2} \text{am}^{-1}$	R 5–16 μm
H_2O	29.0	2.69 (ν_1, ν_3)	200	130	6.27 (ν_2)	250	55
HDO	18.2	3.67 ($\nu_{1,2}, \nu_2$)	270	150	7.13 (ν_2)		77
CH_4	10.0	3.31 (ν_3)	300	300	7.66 (ν_4)	140	130
CH_3D	7.8	4.54 (ν_2)	25	280	8.66 (ν_6)	119	150
NH_3	20.0	2.90 (ν_3)	13	170	10.33	600	50
		3.00 (ν_1)	20		10.72 (ν_2)		
PH_3	8.9	4.30 (ν_1, ν_3)	520	260	8.94 (ν_4)	102	126
					10.08 (ν_2)	82	110
CO	3.8	4.67 (1-0)	241	565			
CO_2	1.6	4.25 (ν_1)	4100	1470	14.99 (ν_2)	220	420
HCN	3.0	3.02 (ν_3)	240	1100	14.04 (ν_2)	204	240
C_2H_2	2.3	3.03 (ν_3)	105	1435	13.7 (ν_5)	582	320
C_2H_6	1.3	3.35 (ν_7)	538	2300	12.16 (ν_{12})	36	635
O_3	0.9				9.60 (ν_3)	348	1160

Table 2: Main molecular signatures and constraints on the spectral resolving power (from Tinetti, Encrenaz, Coustenis, 2013). $\Delta\nu$ is the spectral interval between two adjacent J-components of a band. S_{max} is the intensity of the strongest band available in the spectral interval. R is the spectral resolving power required to separate two adjacent J-components ($\Delta\nu$). Rotational constants, bands assignments and intensities are taken from Herzberg (1968), Townes and Schawlow (1975), Pugh and Rao (1976) and Rothman et al. (1983). Note that the unit “am” stands for amagat.

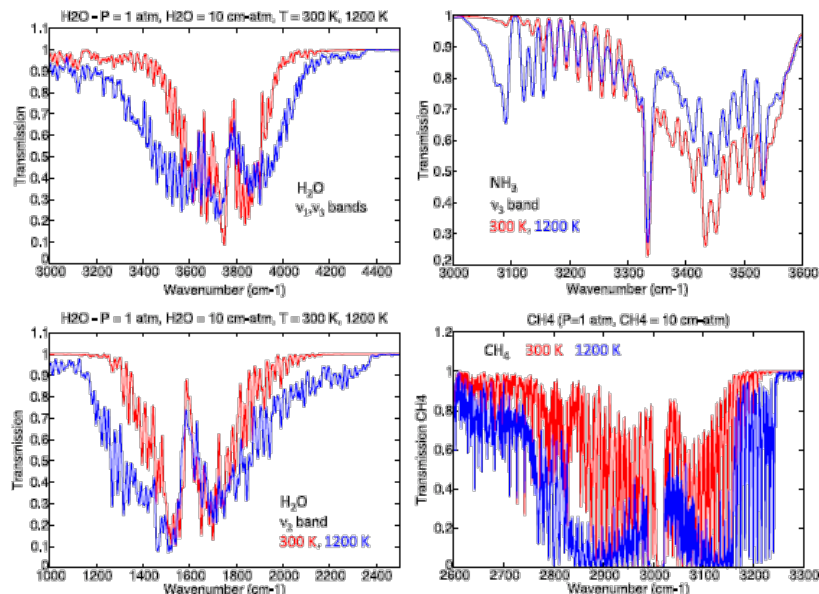


Fig. 2-1: Examples of synthetic spectra of H_2O , NH_3 and CH_4 in some of their fundamental bands, for two temperatures (300 K and 1200 K) [from Tinetti, Encrenaz, Coustenis, 2013]. The spectral resolution is 10 cm^{-1} , corresponding to a resolving power of 100 at $10 \mu\text{m}$ ($\text{NH}_3 \text{ v}_2$ band), 150 at $6 \mu\text{m}$ ($\text{H}_2\text{O} \text{ v}_2$ band) and 300 around $3 \mu\text{m}$ ($\text{H}_2\text{O} \text{ v}_1$ and v_3 bands, $\text{CH}_4 \text{ v}_3$ band). In all cases, the resolving power is sufficient to separate two adjacent J-components in each band.

The spectral features are broadened at high temperature, due to the increasing contribution of high J-value components in each molecular band (see Fig. 2-1 and Appendix). On one hand they are detectable at lower spectral resolution, but if multiple molecular species overlap the identification becomes more difficult and additional spectral features in other part of the spectrum might be needed to confirm a detection. Figure 2-2 shows the transmission of H_2O , CO , CO_2 , CH_4 and NH_3 between 1 and $16 \mu\text{m}$. At hot temperatures, even at spectral resolving power $R > 30$ at the long wavelengths it is still possible to identify the main species, but we lose the possibility to resolve the CO_2 , HCN and other hydrocarbons Q-branches.

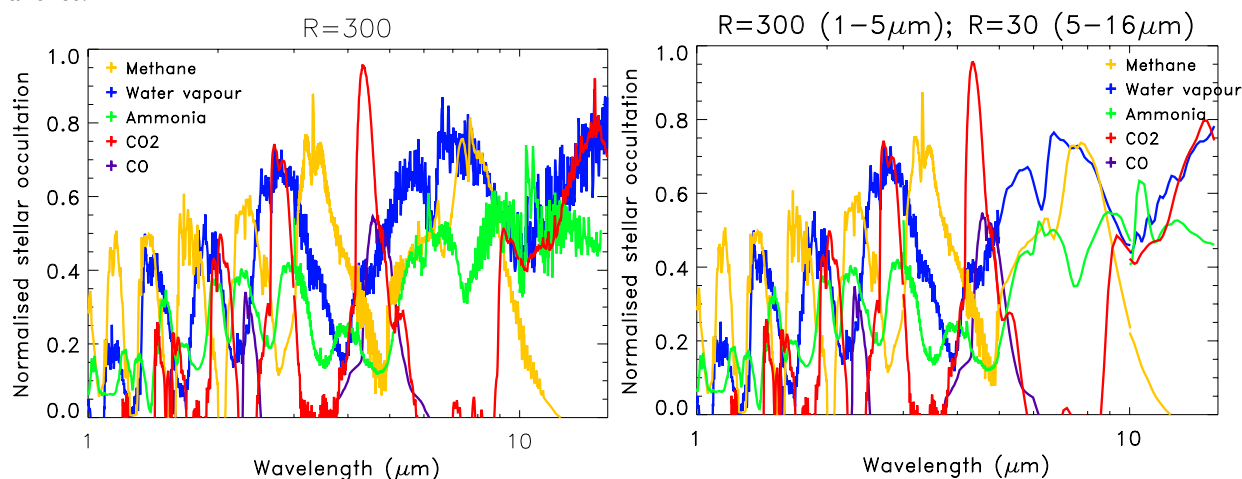


Fig. 2-2: Simulated transmission spectra of a gaseous exoplanet at 800 K (i.e. not too hot or too cold). The spectra were generated at a constant spectral resolving power $R = 300$ (left), and at an optimal resolving power $R=300$ for $\lambda <$

5 μm and $R=30$ for $\lambda > 5 \mu\text{m}$ (right). Especially at the high temperatures, where broadening occurs, the latter solution is sufficient for the detection of the key molecules at long wavelengths, through their Q, P or R branches.

2.2 The 1 – 2 μm range

While many transit spectra of hot Jupiters have been observed in this spectral range using HST/NICMOS, HST/WFC3 and ground-based facilities, modelling exoplanetary spectra in this spectral range is complicated by the complexity of the molecular signatures. Many weak bands (typically overtone and combination bands) are present between 1 and 2 μm . Their spectroscopic identification is not complete, and the calculation of the opacities at high temperature is much more uncertain than at longer wavelengths (see Tennyson & Yurchenko, TN). It should be emphasized that many molecular transitions are still missing in databases such as GEISA or HITRAN, especially in this wavelength interval.

Metal oxides and hydrides, on the contrary, have important spectral features in this region, mainly due to electronic transition (see Fig. 2-3).

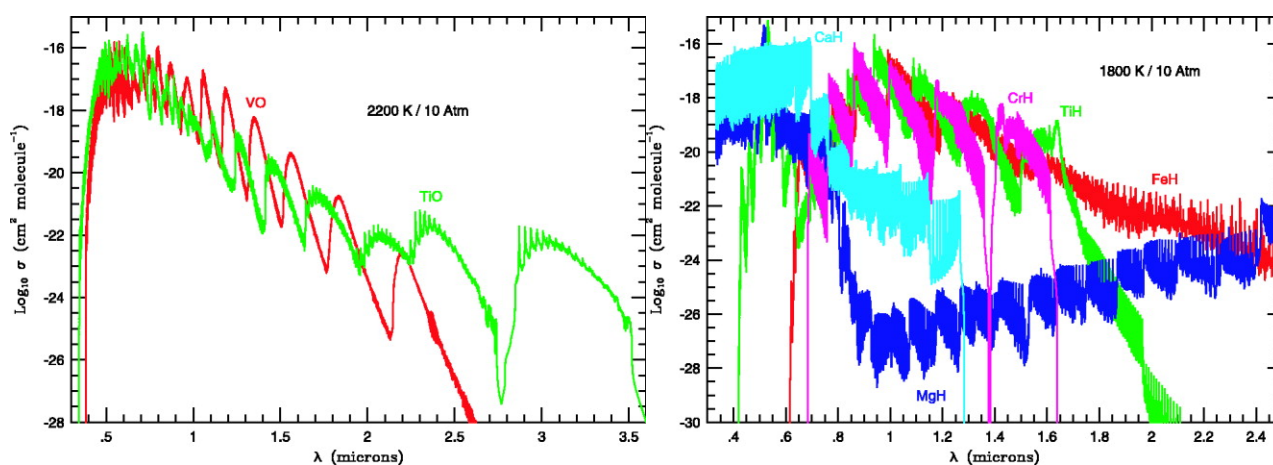


Fig. 2-3: Absorption by metal oxides and hydrides as a function of wavelength at a fixed temperature and pressure, from Sharp & Burrows (2007).

2.3 The 1 – 16 μm range

As a summary of the above discussion, Figures 2-4 show models of the expected contributions of a large number of molecules to the transit/eclipse spectrum of a hot gaseous exoplanet between 1 and 16 μm . The atmospheric temperature is assumed = 800K. Since we are interested in the relative molecular contributions here, the atmospheric absorption is normalised to 1; typically the fraction of stellar flux absorbed by the atmosphere of a hot planet is 10^{-4} - 10^{-3} . In addition to the main candidate absorbers (H_2O , CH_4 , NH_3 , CO , CO_2), calculations include contributions from HCN , O_3 , H_2S , PH_3 , SO_2 , C_2H_2 , C_2H_6 and H_3^+ .

In Figure 2-4, two values (300 and 30) are used for the spectral resolving power. It is worth noticing the possible signature of H_3^+ around 2 μm and 3-4 μm , easily detectable with a resolving power of ~ 300 . The H_3^+ ion, which plays a critical role in the cooling and stabilising of gaseous planets' atmospheres (Maillard and Miller, 2012), has been detected in the ionospheres of Jupiter, Saturn and Uranus (Drossart et al., 1989; Geballe et al., 1993; Trafton et al., 1993), and its presence could be reasonably expected in the upper atmospheres of highly irradiated gaseous planets (Koskinen et al. 2007). While $R=30$ is ok to detect most of the molecules at $\lambda > 5 \mu\text{m}$, especially at high temperatures, we would lose the possibility to resolve the CO_2 , HCN and other hydrocarbons Q-branches between 11 and 16 μm .

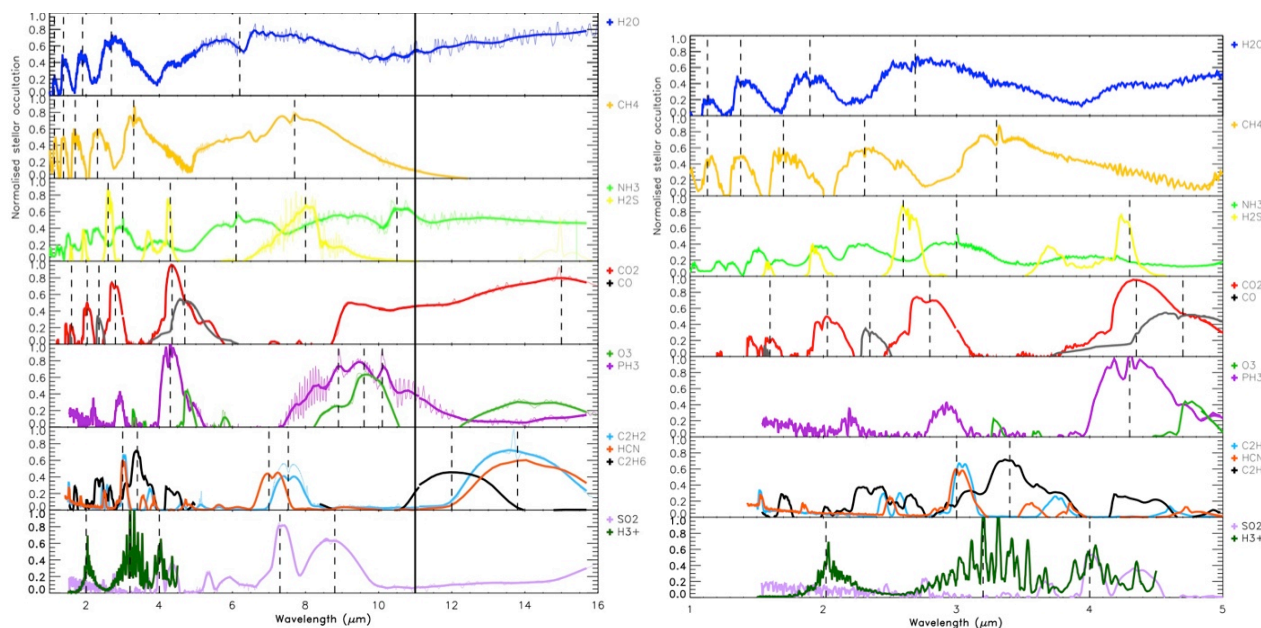


Fig. 2-4: Absorption contributions from different molecules in the transmission spectrum of a hot, gaseous exoplanet. Two values of the spectral resolving power are used: 300 (thin line) and 30 (thick line). The dashed vertical lines indicate the positions of maximum absorption for the different molecules. The thick, black vertical line separate the EChO required spectral coverage (11 μm) from the goal (16 μm). We used high temperature line lists BT2 (Barber et al., 2006) for water, BYTe (Yurchenko et al, 2011) for ammonia, Neale et al. (1996) coefficients for H_3^+ and HITEMP (Rothman et al. 2010) for CO and CO_2 . The other molecules were simulated using HITRAN 2012 (Rothman et al. 2013) line list. Right: enlargement of fig. on the left in the 1 – 5 μm range, for a spectral resolving power of 300.

3 WAVELENGTHS LESS THAN 1 μm

The portion of stellar flux reflected/scattered by the planet peaks in the UV, visible or near-infrared, depending on the spectral type of the host star. It is essential to measure both the reflected flux and the thermal emission from the planet to estimate the energy budget correctly.

For hot planets, opacities in the visible range are dominated by metallic resonance lines (Na at 0.59 μm , K at 0.77 μm , and weaker Cs transitions at 0.85 and 0.89 μm). Theoretical calculations of absorption profiles of Na, K, Cs, Rb perturbed by H_2 and He at high temperatures have been performed by Allard et al. (2002; 2006). Metal oxides and hydrides also may play an important role (Fig. 2-3).

Figure 3-1 shows a simulated visible spectrum of a gaseous, cloud-free exoplanet at spectral resolving power $R \sim 200$. For cloud-free atmospheres, a resolving power of ~ 100 is still sufficient for identifying the resonance lines of Na and K, but not to resolve the centre of the line. Atomic species such as HeI, Ca and Fe have been sought in hot Jupiters atmospheres, but not yet detected in exoplanets.

In a cloud-free atmosphere, the continuum in the UV-VIS is given by Rayleigh scattering on the blue side, i.e. for wavelengths shorter than 1 micron (Rayleigh scattering varies as $1/\lambda^4$). If there are clouds or hazes with small-size particles, those should be detectable in the visible (de Kok and Stam, 2012). For small (particle diameter $a \ll \lambda$), spherical particles the multiple scattering with the stellar photons can be simulated using Mie scattering approximation (e.g. Goody and Yung, 1989). If the particles are larger (particle diameter $a \geq \lambda$) or non-spherical, then the calculations are more complex (Liou, 2002). Apart from the particle size and shape, the other important parameters are the particle

distribution function and the pressure of the atmospheric layer where clouds/hazes form. From a radiative transfer perspective, the composition is less important and this explains why it is exceedingly difficult to retrieve cloud or haze composition from remote sensing observations.

Finally, as mentioned previously, the visible range is important to estimate and correct for the contribution of the stellar activity (Ribas, Micela and Tinetti, TN).

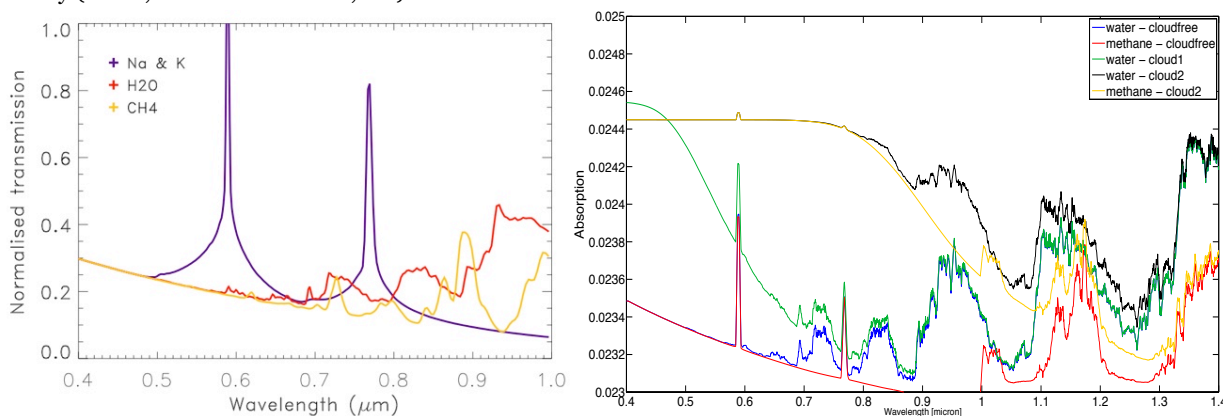


Fig. 3-1: Left: Synthetic transit spectra of a hot, gaseous exoplanet in the visible range, assuming a spectral resolving power $R \sim 200$. The resonance lines are Na at $0.59 \mu\text{m}$ and K at $0.77 \mu\text{m}$ (calculated cross sections from Allard et al., 2003). Water vapour and methane spectral features are weaker here compared to the IR. We used calculated BT2 line list for water at high temperature (Barber et al., 2006) and methane absorption coefficients from Karkoschka & Tomasko (2010). The slope of the continuum is due to Rayleigh scattering by molecular hydrogen. Right: comparison between cloud-free and cloudy atmospheres for a hot-Jupiter (Hollis et al., 2013). The cloudy spectra are differentiated by the particle size, thickness, level of the atmosphere at which they occur etc. The spectral resolving power is $R \sim 300$.

4 CONCLUSIONS

1. A broad wavelength coverage is required to:
 - capture the variety of planets at different temperatures
 - detect the variety of chemical components present in exoplanet atmospheres
 - guarantee redundancy (i.e. molecules detected in multiple bands of the spectrum) to improve the reliability of the detection – especially when multiple chemical species overlap in a particular spectral range.
 - enable an optimal retrieval of the chemical abundances and thermal profile
2. The required wavelength coverage $0.55\text{--}11 \mu\text{m}$ for EChO, will guarantee that ALL the key chemical species (H_2O , CH_4 , CO , CO_2 , NH_3) and ALL other species (Na, K, VO, TiO, TiH, CrH, H_2S , SO_2 , SiO, H_3^+ , C_2H_2 , C_2H_4 , C_2H_6 , PH_3 , HCN etc.) can be detected – if present and with the appropriate SNR – in ALL the exoplanet types observed by EChO, with the exception of CO_2 and C_2H_6 in temperate planetary atmospheres. The limit at $0.55 \mu\text{m}$ is given by Na, which absorbs at $0.59 \mu\text{m}$. The boundary at $\sim 11 \mu\text{m}$ is given by NH_3 , whose absorption is centred at $10.5 \mu\text{m}$ (see Tessenyi and Tinetti TN).
3. The required wavelength range $0.55\text{--}11 \mu\text{m}$, will guarantee the retrieval of molecular abundances and thermal profiles, especially for gaseous planets, with an increasing difficulty in retrieving said information for colder atmospheres



4. The extension to 16 μm , on top of the required coverage, would guarantee that CO_2 and C_2H_6 can be detected in temperate planetary atmospheres. It will also offer the possibility of detecting additional absorption features for HCN, C_2H_2 , CO_2 and C_2H_6 for all other planets and improve the retrieval of thermal profile (Barstow et al. TN).
5. The extension to 0.4 μm on top of the required coverage, although non-critical, would improve the detection of Rayleigh scattering/cloud contribution (Fig. 3-1 right) and stellar characterisation.
6. A spectral resolving power $R = 300$ for $\lambda < 5 \mu\text{m}$ will permit the detection of most molecules/atoms at any temperature. At $\lambda > 5 \mu\text{m}$, $R = 30$ is enough to detect the key molecules at hot temperatures, due to broadening. For temperate planets, $R = 30$ at longer wavelengths is also an optimal solution, given there are fewer photons.

5 REFERENCES

1. Allard F., *Spectra of early and late type stars*, ECHO-TN-0001-ENS
2. Allard NF, Spiegelman F (2006) *Collisional line profiles of rubidium and cesium perturbed by helium and molecular hydrogen*. *Astron Astrophys* 452:351–356
3. Allard NF, Allard F, Hauschildt PH, Kielkopf JF, Machin L (2003) *Astron Astrophys* 411:L473
4. Barber RJ, Miller S, Tennyson J, Harris GJ, Tolchenov RN (2006) *Mon Not R Astron Soc* 368:1087–1094
5. Barstow et al (2013) *On the potential of the EChO mission to characterise gas giant atmospheres*. *Mon Not R Astron Soc*, 430 (2013) 1188-1207-1188-1207.
6. Barstow et al. a, *Retrieval techniques*, ECHO-TN-0001-OXF
7. Barstow et al., *On the importance of LWIR for spectral retrieval*, ECHO-TN-0002-OXF
8. De Kok RJ, Stam DM (2012) *The influence of forward-scattered light in transmission measurements of (exo)planetary atmospheres*. *Icarus* 221(2):517–524
9. Drossart et al., 1989, Drossart, P. et al., Detection of $\text{H}_3(+)$ on Jupiter, *Nature* (ISSN 0028-0836), vol. 340, Aug. 17, 1989, p. 539-541.
10. Geballe et al., 1993, Geballe, T. R.; Jagod, M.-F.; Oka, T., Detection of $\text{H}_3(+)$ infrared emission lines in Saturn, *Astrophysical Journal, Part 2 - Letters* (ISSN 0004-637X), vol. 408, no. 2, p. L109-L112.
11. Goody RM, Yung YL (1989) *Atmospheric radiation: theoretical basis*. Oxford University Press, London
12. Hollis MDJ, Tessenyi M, Tinetti G (2013) *Tau: A 1D radiative transfer code for transmission spectroscopy of extrasolar planet atmospheres*, *Computer Physics Communications*, 184(10), 2351 - 2361.
13. Koskinen et al. 2007, Koskinen, T., Aylward, A. & Miller, S. 2007 A stability limit for the atmospheres of giant extrasolar planets. *Nature*, 450, 845–848.
14. Liou K. N. (2002) *An introduction to atmospheric radiation*, 2nd edn. International geophysics series, vol 84. Academic Press, San Diego. 583 pp.
15. Maillard and Miller, 2012, *The molecular ion H^+_3 in emission in planetary atmospheres*, ASP conference “Molecules in the atmosphere of an exoplanet”, Beaulieu, Dieters, Tinetti, Paris, 2008
16. Moses, J., Visscher, C., Fortney, J., et al. (2011), *ApJ*, 737, 15.



17. Neale et al., 1996, Neale L., Miller S., Tennyson J., ApJ, 464, 516
18. Ribas, I., Micela, G. and Tinetti, G. (2013) TN, *Correcting for Stellar Activity*, EChO-SRE-SA-PhaseA-002
19. Rothman LS et al (2009) *The HITRAN 2008 molecular spectroscopic database*. J Quant Spectrosc Radiat Transf 110:533–572
20. Rothman L. S. et al., 2010, *HITEMP* J. Quant. Spectrosc. Radiat. Transf., 111, 2139.
21. Rothman, L. S., I.E. Gordon, Y. Babikov, A. Barbe, D.Chris Benner, P.F. Bernath, et al, *The HITRAN 2012 molecular spectroscopic database*, JQSRT (in press) (2013). DOI: 10.1016/j.jqsrt.2013.07.002.
22. Sharp C. M. & A. Burrows, 2007, *Atomic and molecular opacities for Brown Dwarf and giant planet atmospheres*, The Astrophysical Journal Supplement Series, 168:140-166.
23. Tennyson J, Yurchenko S (2012) *ExoMol: molecular line lists for exoplanet and other atmospheres*. Mon Not R Astron Soc 425:21
24. Tennyson J, Yurchenko S., *The Status of Spectroscopic Data for the EChO Mission*, ECHO-TN-0008-UCL
25. Tessenyi M et al (2013) *Molecular detectability in exoplanetary emission spectra*. Icarus, 26, 1654–1672.
26. Tessenyi M and Tinetti G, *NH₃ detectability: 11 μ m vs 10.6 μ m cutoff*, ECHO-TN-0005-UCL
27. Tinetti, Encrenaz, Coustenis, *Spectroscopy of planetary atmospheres in our Galaxy*, Astron Astrophys Rev (2013) 21:63
28. Trafton et al., 1993, Trafton, L. M.; Geballe, T. R.; Miller, S.; Tennyson, J.; Ballester, G. E.; *Detection of H₃⁺ from Uranus*, Astrophysical Journal, Part 1 (ISSN 0004-637X), vol. 405, no. 2, p. 761-766.
29. Venot, O., Hébrard, E., Agundez, M., et al. 2012, A&A, 546, A43
30. Venot O., et al. 2013, *The atmospheric chemistry of the warm Neptune GJ3470b*, A&A Submitted
31. Yurchenko SN, Barber RJ, Tennyson J (2011) *A variationally computed line list for hot NH₃*. Mon Not R Astron Soc 413:1828

6 APPENDIX

We show in this appendix simulated emission spectra for a range of planetary classes, molecular types and molecular mixing ratios. The spectra are shown at a spectral resolving power of few hundreds. We present in the main text the effects of degrading the spectral resolving power.

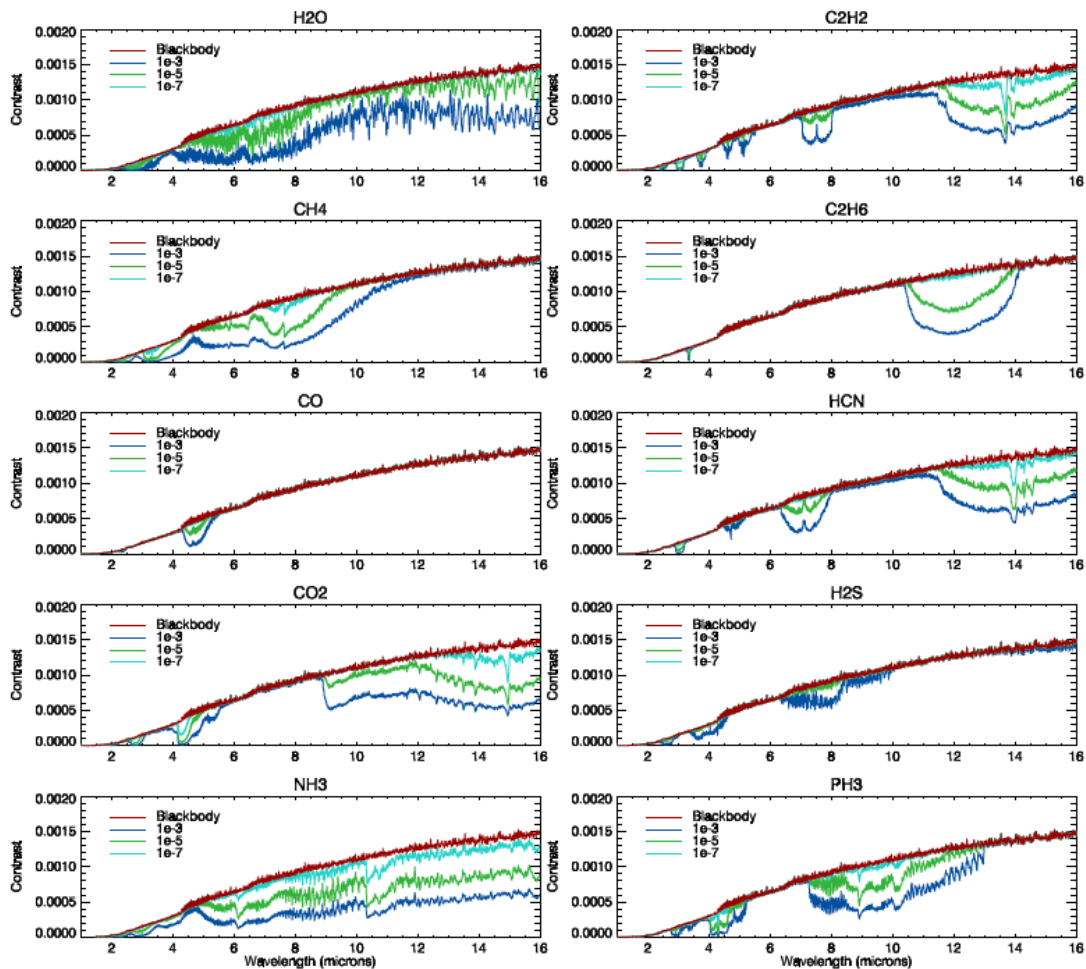


Fig. A-1: Eclipse spectra for a warm Neptune (Tessenyi et al., 2013): planet/star contrast spectra simulating the effect of the 10 considered molecules: CH_4 , CO , CO_2 , NH_3 , H_2O , C_2H_2 , C_2H_6 , HCN , H_2S and PH_3 . The red line shows a planetary blackbody emission with no molecules present, divided by a stellar spectrum. The green-blue coloured lines depict the molecular features at different mixing ratios.

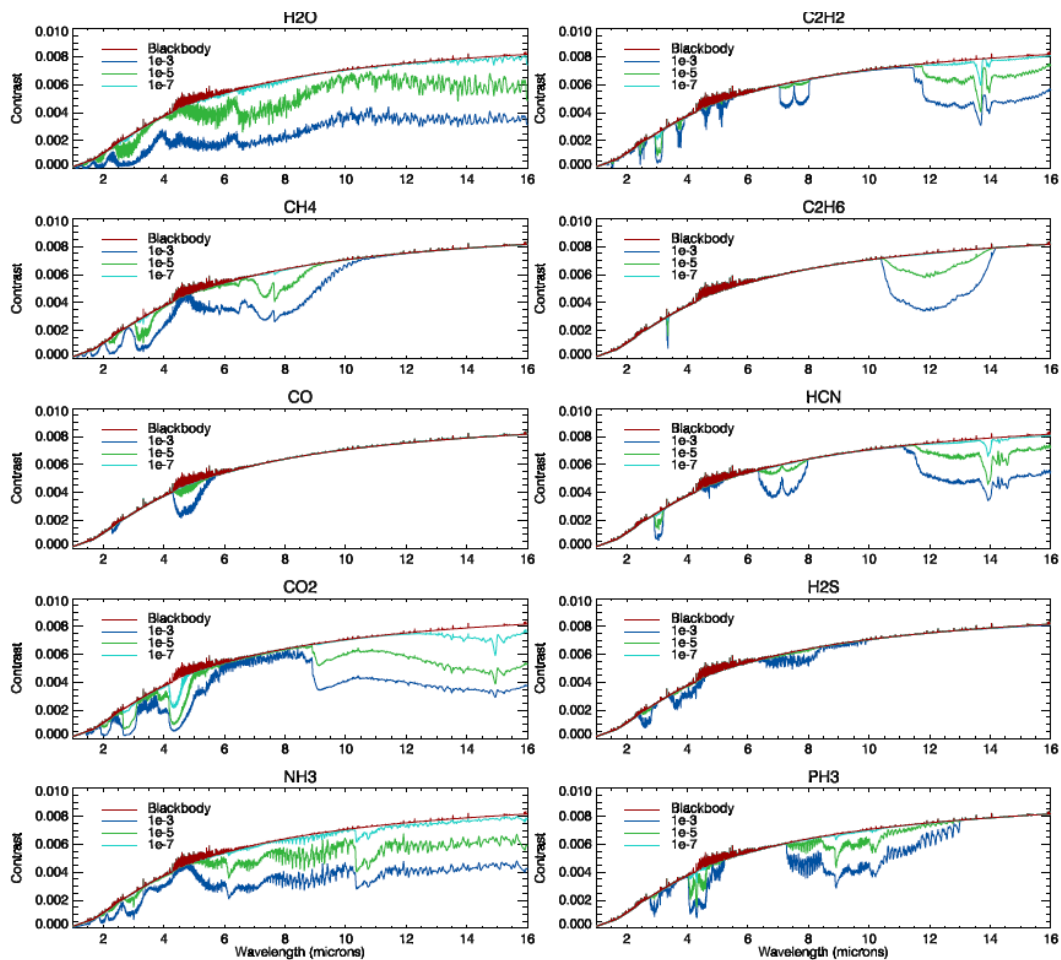


Fig. A-2: Eclipse spectra for a hot Jupiter (Tessenyi et al., 2013): planet/star contrast spectra simulating the effect of the 10 considered molecules: CH_4 , CO , CO_2 , NH_3 , H_2O , C_2H_2 , C_2H_6 , HCN , H_2S and PH_3 . The red line shows a planetary blackbody emission with no molecules present, divided by a stellar spectrum. The green-blue coloured lines depict the molecular features at different mixing ratios.

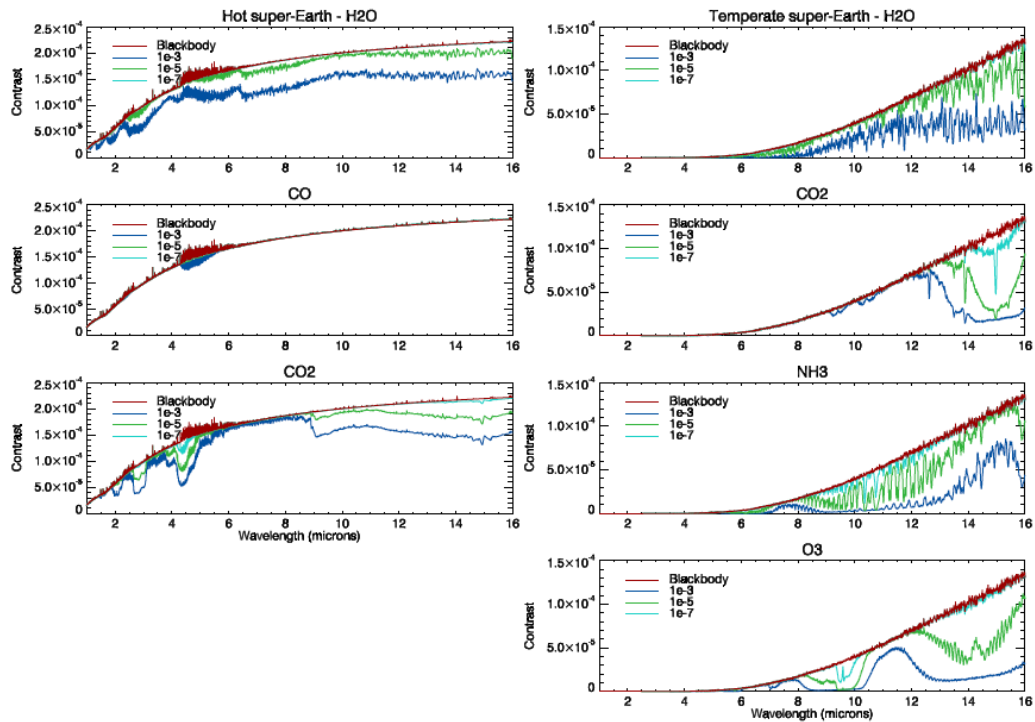


Fig. A-3: Hot (left) and temperate (right) super-Earth (fig. from Tessenyi et al., 2013): planet/star contrast spectra simulating the effect of the considered molecules: H_2O , CO and CO_2 for the hot planet, and H_2O , CO_2 , NH_3 and O_3 for the temperate case. The red line shows a planetary blackbody emission with no molecules present, divided by a stellar spectrum. The green-blue coloured lines depict the molecule features at varying abundances. For clarity purposes, only three abundances are plotted out of the five calculated.

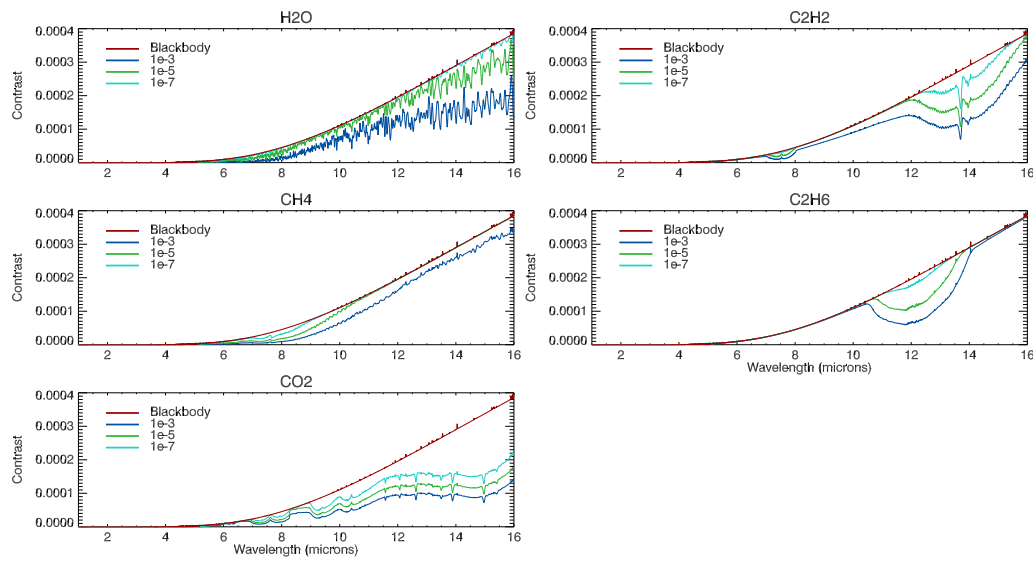


Fig. A-4: *Temperate Jupiter: planet/star contrast spectra simulating the effect of the 5 considered molecules: H₂O, CH₄, CO₂, C₂H₂ and C₂H₆. The red line shows a planetary blackbody emission with no molecules present, divided by a stellar spectrum. The green-blue coloured lines depict the molecule features at varying abundances. For clarity purposes, only three abundances are plotted out of the five calculated.*